Electronic Supplementary Material (ESI) for Inorganic Chemistry Frontiers.

Supporting Information Section

Construction of superhydrophobic microenvironment via polystyrene coating: an unexpected way to stabilize Cu^{I} against oxidation

*Yu-Xia Li, Yu-Nong Ji, Shi-Xian Mao, Meng-Meng Jin, Xiao-Qin Liu, and Lin-Bing Sun**

State Key Laboratory of Materials-Oriented Chemical Engineering, Jiangsu National Synergetic Innovation Center for Advanced Materials (SICAM), College of Chemical Engineering, Nanjing Tech University, 30 South Puzhu Road, Nanjing 211816, China.

*Corresponding author.

E-mail address: lbsun@njtech.edu.cn (L.-B. Sun)

Materials characterization

XRD patterns of the materials were gained in the 2 θ range from 5° to 60° on a Bruker D8 Advance diffractometer with Cu Kα radiation at 40 kV and 40 mA. The N_2 adsorption isotherm was measured at −196 °C using an ASAP 2020 instrument. Ahead of analysis, the samples were degassed at 150 °C for 4 h under vacuum. The BET surface area was computed at relative pressure ranging from 0.05 to 0.20. The total pore volume was calculated from the amount adsorbed at a relative pressure of about 0.99. Field-emission scanning electron microscope (SEM) was executed on a HITACHIS-4800 to observe the morphologies of the materials. High-resolution transmission electron microscopy (HRTEM) was executed on a JEM-2010UHR electron microscope at 200 kV. FT-IR measurements were performed on a NicoletS-4 Nexus 470 spectrometer using the KBr pellet technique. The spectra were gathered with a 2 cm^{-1} resolution. Thermogravimetric (TG) analyses were performed using a thermobalance (STA-499C, NETZSCH). The analyte was heated from room temperature (~25 °C) to 800 °C at a rate of 10 °C/min using platinum pans under a flow of air gas. Analyses of the polystyrene were performed on a Shimadzu gel permeation chromatography (GPC) with a molecular weight range coverage of 1,000,000 to 92 Da. Tetrahydrofuran was used as the solvent and the sample concentrations were adjusted to be ~1–1.8 mg/mL. GPC was performed in the batch processing mode with a solvent flow rate of 1 mL/min and the spectra were obtained using a diode array UV-vis detector at 259 nm wavelength. These GPC analyses were performed using Shimadzu LCsolution software. The water contact angle was measured by static drop method on the model DROPMETER A-100P video optical contact angle measuring instrument. After pressing, the sample is placed on the platform and a drop of water is added to calculate the contact angle. The

accuracy of water contact angle measurement is 1 degree. X-ray photoelectron spectroscopy (XPS) analysis was carried on a Physical Electronic PHI-550 spectrometer equipped with an Al Kα X-ray source (1486.6 eV) at 10 kV and 35 mA. Quantitative analysis of Cu^{I} content was calculated by a wet chemistry titration method.[1] UV-vis spectra were gained using the Cintra 20 (Australian) spectrometer in the reflection mode. The spectra of samples were obtained in the wavelength range of 250–800 nm at intervals of 1 nm with a $BaSO_4$ reflectance standard used as the baseline. For the evaluation of the long-term stability of Cu^{I}, Cu^{I}-containing samples were placed in a container containing a saturated solution of NaCl at room temperature with RH=75% to accelerate the oxidation of Cu^{I}. The exposed samples were characterized at different intervals.

ADS experiments

The model fuel used for ADS experiments was prepared by mixing thiophene, BT, or DMDBT with isooctane, and the sulfur content was ~550 ppmw. Moisture is present in all commercial fuels. In order to test the effect of moisture on desulfurization capacity, the model fuel containing 550 ppmw thiophene in isooctane was mixed and thoroughly agitated with 300 ppmw water. ADS experiments were performed in a vertical quartz column at room temperature. The model fuel was allowed to contact the adsorbent pumped up with a mini creep pump at the rate of 3 mL/h. Adsorbents were pretreated in flowing Ar at 150 °C for 4 h followed by cooling to room temperature. Effluent solutions were collected periodically until saturation was reached. The sulfur content of effluent solutions was analyzed using a Varian 3800 gas chromatograph (GC) equipped with a pulsed-flame photometric detector (PFPD). A calibration curve was prepared to verify the GC results.

Breakthrough curves were generated by plotting the normalized sulfur concentration versus the cumulative fuel volume, which was normalized by the adsorbent weight. The normalized sulfur concentration (c/c_0) was obtained by measuring the ratio of the detected sulfur content (c) to that of the initial sulfur content (c_0). The adsorption capacity was obtained from integral calculus.

Table S1 Textual properties and elemental composition of samples

Sample	S_{BET} (m^2/g)	V_p (cm^3/g)	Elemental content (*wt*%) C	Elemental content (*wt*%) H	PS content (*wt*%)
MIL-101(Cr)	3332	1.87	31.0	4.6	-
$Cu^{I}M$	2058	1.06	26.0	4.8	-
$Cu^{I}M$@PS-1.5	1751	0.89	28.9	5.0	4.4
$Cu^{I}M$@PS-2	1918	0.97	30.8	5.1	7.2
$Cu^{I}M$@PS-2.5	1549	0.81	31.9	5.1	8.8
$Cu^{I}M$@PS-r	1608	0.80	30.6	5.1	6.9

Table S2 GPC data for PS after polymerization of styrene

Sample	M_n	M_w	M_w/M_n
PS-1.5h	5786	81550	14.1
PS-2h	6668	84987	12.7
PS-2.5h	7505	116790	15.6
$Cu^{I}M$@PS-1.5	68767	151348	2.20
$Cu^{I}M$@PS-2	92542	167169	1.81
$Cu^{I}M$@PS-2.5	125502	230094	1.83

Table S3 Effects of moisture on the desulfurization capacity of the adsorbents

Adsorbent	Adsorption capacity for fuel without H_2O (mmol/g)	Adsorption capacity for fuel with H_2O (mmol/g)	Concentration of H_2O additive in the fuel	Ref.
Cu^IM@PS-2	0.208	0.202	300 ppmw	This work
Cu^IM	0.210	0.079	300 ppmw	This work
Cu(I)Y	0.168[a]	0.0265[a]	300 ppmw	2
AC-WPH	0.0130	0.0122	56 ppmw	3
Cu(I)Y@P(3.1%)	0.537[a]	0.535[a]	300 ppmw	4
Zn/Ni/Cu-BTC	0.0300	0.0145	500 ppmw	5
Zn55/Cu–BTC	0.0248	0.0221	water-saturated[b]	6
AC	0.0261	-	0	7
Cu(I)Y	0.548[a]	-	0	4
20Cu/SBA-15	0.155	-	0	8
20 wt % Zn/Al_2O_3	0.0875	-	0	9
MOF-5@AC	0.113	-	0	10
20Ni-MIL-101	0.0689	-	0	11
HP-UiO-66-SO_3Ag	0.233	-	0	12

[a] Breakthrough capacity of sulfur. [b] Model fuel was mixed and thoroughly agitated with distilled water and then the water-saturated simulated oil can be obtained after getting rid of the water phase.

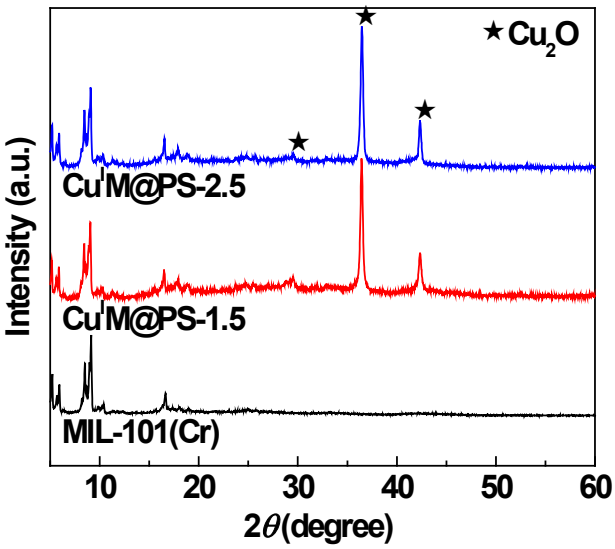

Figure S1 XRD patterns of MIL-101(Cr), $Cu^{I}M$@PS-1.5, and $Cu^{I}M$@PS-2.5.

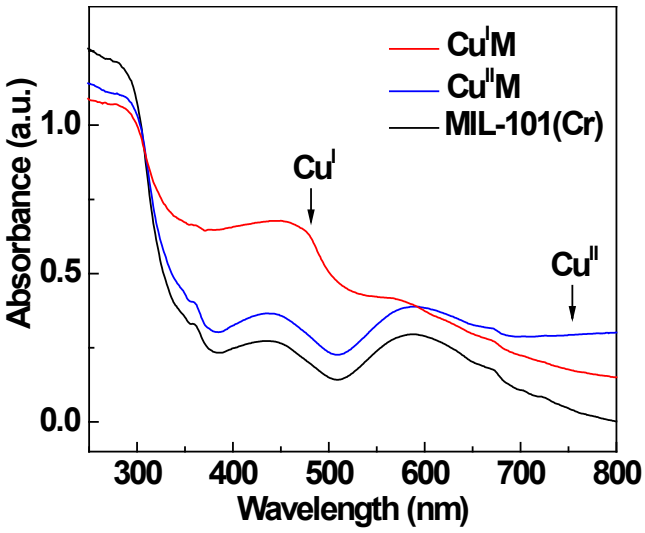

Figure S2 UV-vis absorption spectra of MIL-101(Cr), $Cu^{II}M$, and $Cu^{I}M$.

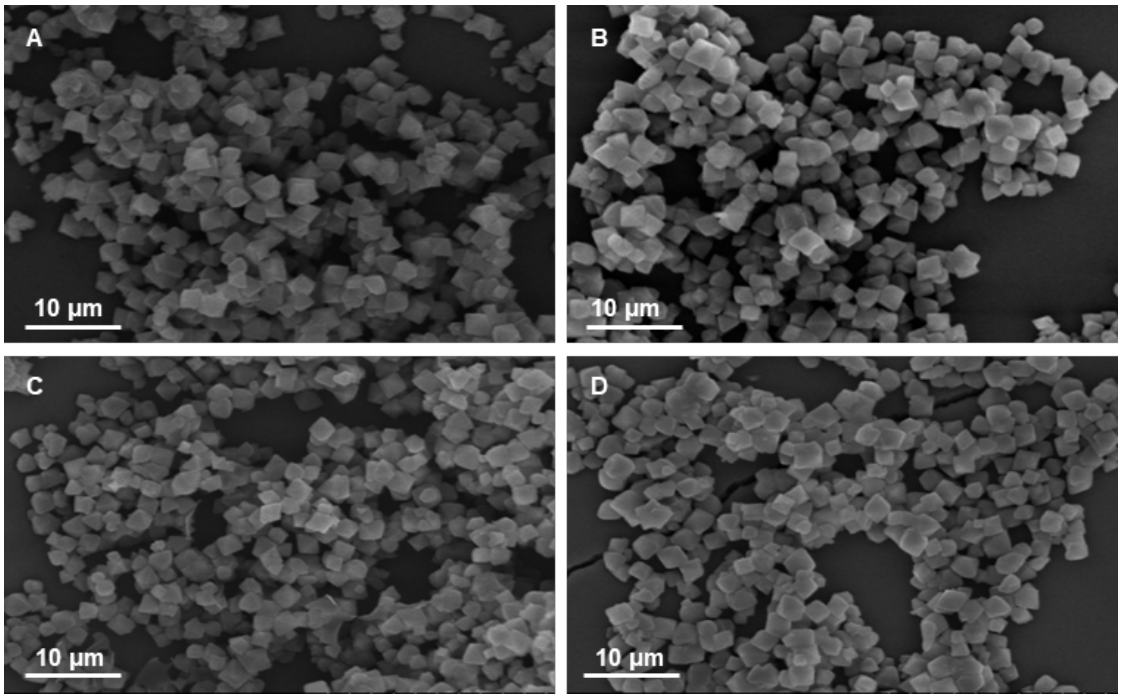

Figure S3 SEM images of (A) $Cu^{I}M$, (B) $Cu^{I}M$@PS-1.5, (C) $Cu^{I}M$@PS-2, and (D) $Cu^{I}M$@PS-2.5.

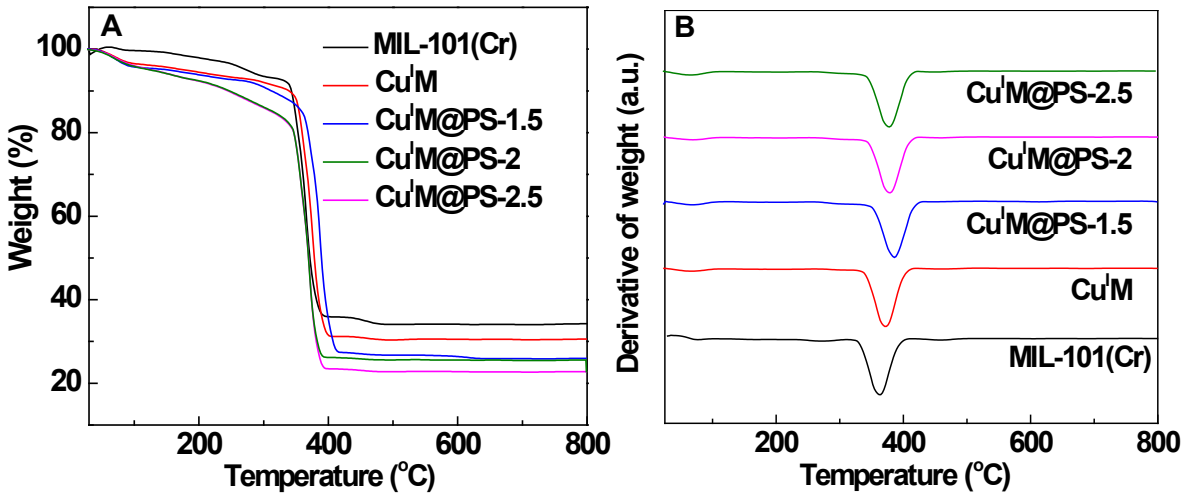

Figure S4 (A) TG and (B) DTG profiles of MIL-101(Cr), Cu^{I}M and Cu^{I}M@PS.

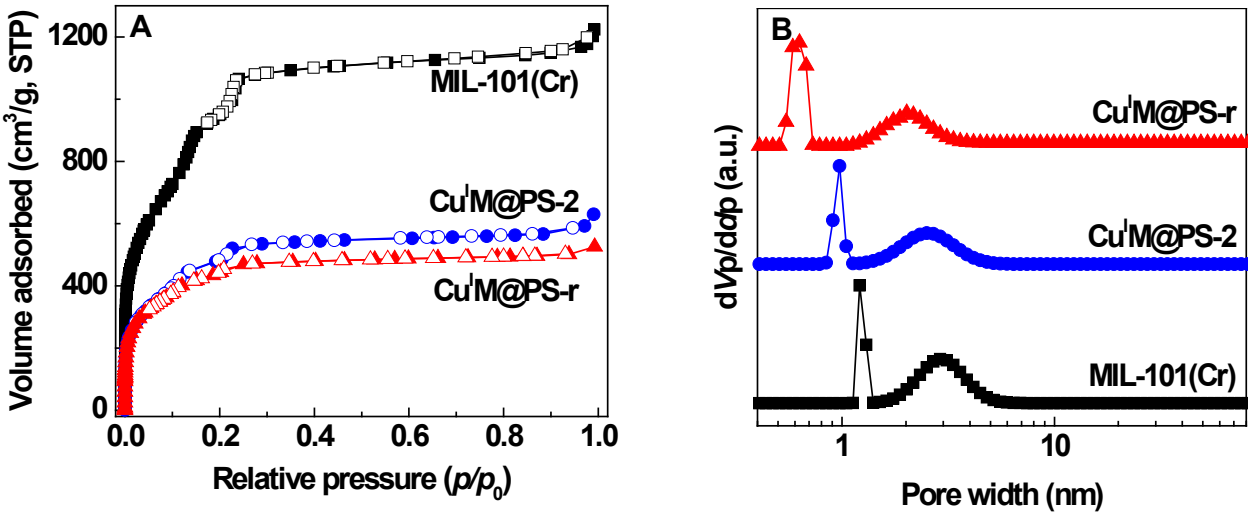

Figure S5 (A) N_2 adsorption-desorption isotherms and (B) pore size distributions of MIL-101(Cr), $Cu^{I}M$@PS-2, and $Cu^{I}M$@PS-r.

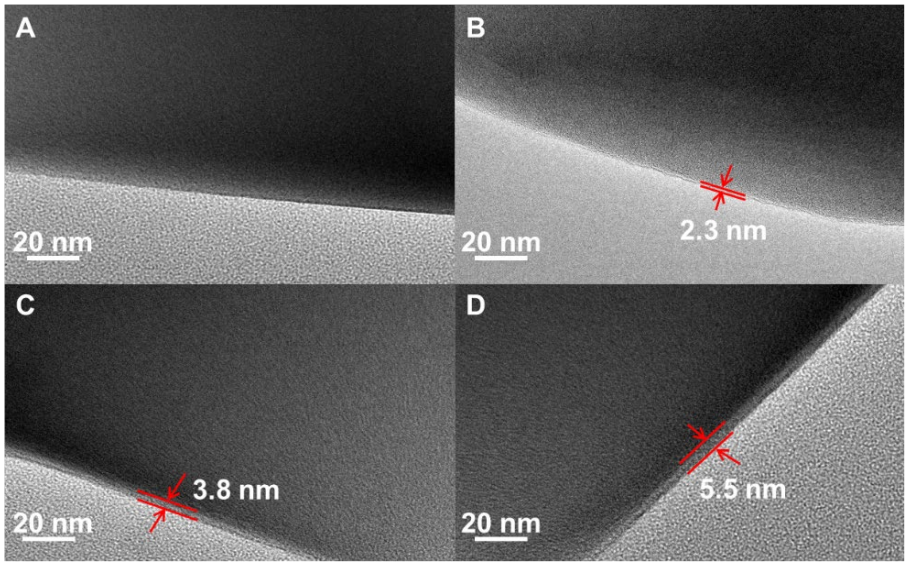

Figure S6 HRTEM images of (A) $Cu^{I}M$, (B) $Cu^{I}M$@PS-1.5, (C) $Cu^{I}M$@PS-2, and (D) $Cu^{I}M$@PS-2.5.

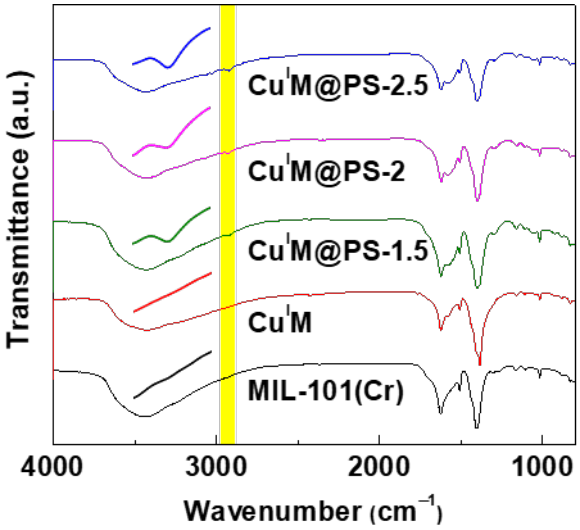

Figure S7 FT-IR spectra of MIL-101(Cr), Cu^{I}M, and Cu^{I}M@PS.

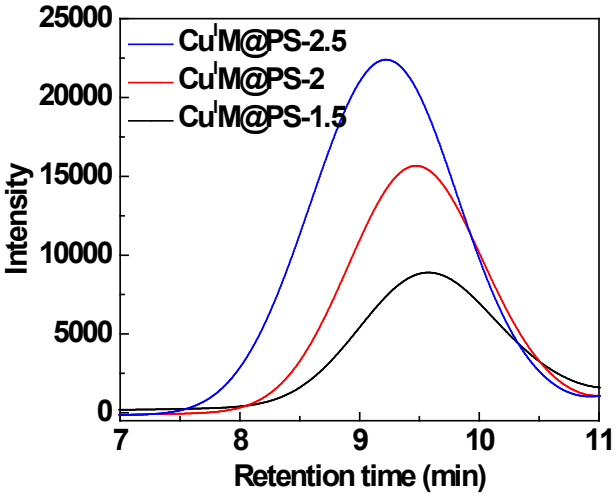

Figure S8 GPC trace of high molecular weight PS in Cu^{I}M@PS.

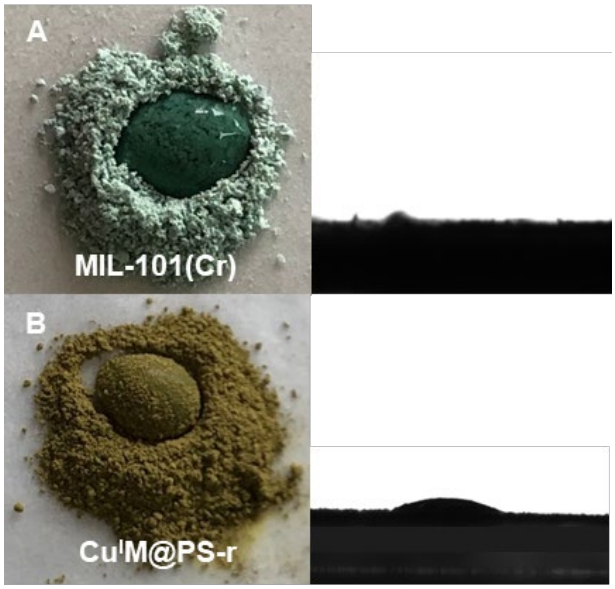

Figure S9 Static water contact angles and pictures of (A) MIL-101(Cr) and (B) Cu^{I}M@PS-r with a drop of water.

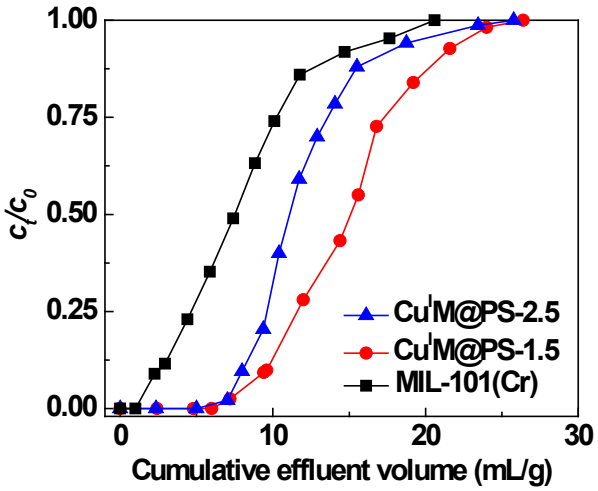

Figure S10 Breakthrough curves of the model fuel containing 550 ppmw thiophene over MIL-101(Cr), Cu^{I}M@PS-1.5, and Cu^{I}M@PS-2.5.

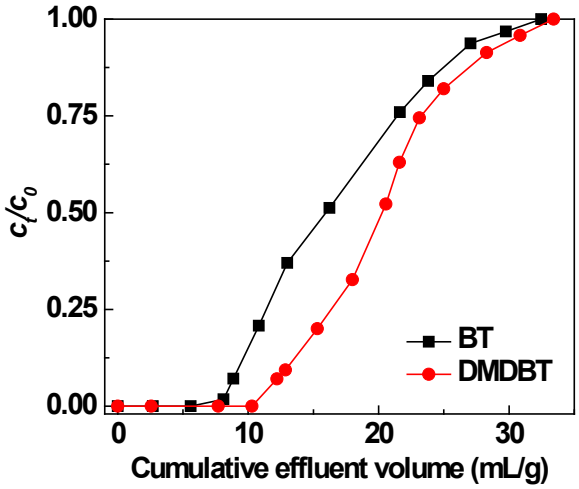

Figure S11 Breakthrough curves of the model fuel containing 550 ppmw BT or DMDBT over $Cu^{I}M$@PS-2.

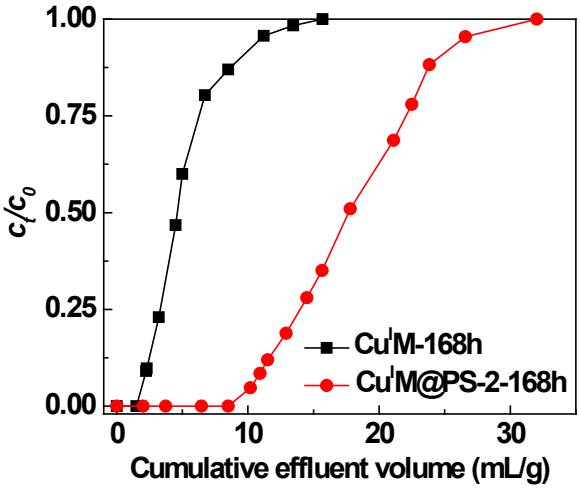

Figure S12 Breakthrough curves of the model fuel containing 550 ppmw thiophene over $Cu^{I}M$ and $Cu^{I}M$@PS-2 after exposure to humid atmosphere with 75% RH for 168 h.

References

1 S.-C. Qi, X.-Y. Qian, Q.-X. He, K.-J. Miao, Y. Jiang, P. Tan, X.-Q. Liu and L.-B. Sun, Generation of hierarchical porosity in metal-organic frameworks by the modulation of cation valence, *Angew. Chem. Int. Ed.*, 2019, **58**, 10104-10109.

2 Y. Li, F. H. Yang, G. Qi and R. T. Yang, Effects of oxygenates and moisture on adsorptive desulfurization of liquid fuels with Cu(I)Y zeolite, *Catal. Today*, 2006, **116**, 512-518.

3 J. Xiao, C. S. Song, X. L. Ma and Z. Lit, Effects of aromatics, diesel additives, nitrogen compounds, and moisture on adsorptive desulfurization of diesel fuel over activated carbon, *Ind. Eng. Chem. Res.*, 2012, **51**, 3436-3443.

4 Y.-X. Li, J.-X. Shen, S.-S. Peng, J.-K. Zhang, J. Wu, X.-Q. Liu and L.-B. Sun, Enhancing oxidation resistance of Cu(I) by tailoring microenvironment in zeolites for efficient adsorptive desulfurization, *Nature Commun.*, 2020, **11**, 3206.

5 T. T. Wang, Y. Y. Fang, W. Dai, L. F. Hu, N. Ma and L. Yu, The remarkable adsorption capacity of zinc/nickel/copper-based metal-organic frameworks for thiophenic sulfurs, *RSC Adv.*, 2016, **6**, 105827-105832.

6 T. T. Wang, X. X. Li, W. Dai, Y. Y. Fang and H. Huang, Enhanced adsorption of dibenzothiophene with zinc/copper-based metal-organic frameworks, *J. Mater. Chem. A*, 2015, **3**, 21044-21050.

7 T. A. Saleh, S. A. Al-Hammadi, A. Tanimu and K. Alhooshani, Ultra-deep adsorptive desulfurization of fuels on cobalt and molybdenum nanoparticles loaded on activated carbon derived from waste rubber, *J. Colloid Interface Sci.*, 2018, **513**, 779-787.

8 F. Subhan, S. Aslam, Z. Yan, L. Zhen, M. Ikram, R. Ullah, U. J. Etim and A. Ahmad, Ammonia assisted functionalization of cuprous oxide within confined spaces of SBA-15 for adsorptive desulfurization, *Chem. Eng. J.*, 2018, **339**, 557-565.

9 X. Yang, C. Cao, K. J. Klabunde, K. L. Hohn and L. E. Erickson, Adsorptive desulfurization with xerogel-derived zinc-based nanocrystalline aluminum oxide, *Ind. Eng. Chem. Res.*, 2007, **46**, 4819-4823.

10 L. Zhu, X. Jia, H. Bian, T. Huo, Z. Duan, Y. Xiang and D. Xia, Structure and adsorptive desulfurization performance of the composite material MOF-5@AC, *New J. Chem.*, 2018, **42**, 3840-3850.

11 S. Aslam, F. Subhan, Z. Yan, U. J. Etim and J. Zeng, Dispersion of nickel nanoparticles in the cages of metal-organic framework: an efficient sorbent for adsorptive removal of thiophene, *Chem. Eng. J.*, 2017, **315**, 469-480.

12 P. Zhang, Y. Xu, K. Guo, Y. Yin, J. Wang and Y. Zeng, Hierarchical-pore UiO-66 modified with Ag^+ for π-complexation adsorption desulfurization, *J. Hazard. Mater.*, 2021, **418**, 126247.